Wiley
Structural Control and Health Monitoring
Volume 2024, Article ID 8880701, 12 pages
https://doi.org/10.1155/2024/8880701

WILEY

Research Article

Evaluation of Vertical Human-Structure Interaction on a Pedestrian Bridge Using a Predictive Human Gait Model

Juan D. Aux[1], **Bryan Castillo**[1], **Carlos Riascos**[2], **Johannio Marulanda**[1] **and Peter Thomson**[1]

[1]*Grupo de Investigación en Ingeniería Sísmica, Eólica, Geotécnica y Estructural, University of Valle, Santiago de Cali, Colombia*
[2]*Construction Technologies Institute, Consiglio Nazionale delle Ricerche, Napoli, Italy*

Correspondence should be addressed to Juan D. Aux; juan.aux@correounivalle.edu.co

Received 27 November 2023; Revised 9 August 2024; Accepted 19 August 2024

Academic Editor: Łukasz Jankowski

Many modern pedestrian bridges exhibit flexibility and susceptibility to vibrations due to the use of lightweight and high-strength materials, which can cause discomfort for pedestrians and affect their serviceability. Although gait biomechanics have been extensively studied and optimisation techniques for gait prediction on rigid surfaces have been previously employed, there is a paucity of studies investigating the effects of human-structure interaction on pedestrian crossings over flexible structures. In this study, inverse dynamics and optimisation techniques were employed to predict human gait on a flexible structure in the sagittal plane. Gait was formulated as an optimal motor task subject to multiple constraints, with the performance criterion being the minimization of mechanical energy expenditure throughout a complete gait cycle. Segmental movements, pedestrian-applied forces, and bridge vibrations were predicted based on parameters describing gait (such as gait speed, gait frequency, and double support duration), as well as physical and dynamic parameters characterizing the pedestrian bridge (including natural frequency, damping coefficient, and bridge length).

1. Introduction

The main source of excitation of pedestrian bridges corresponds to the forces induced by the traffic of people occupying them. However, with the increasing progress in the mechanics of materials linked to current construction trends, architectural designs have focused on the development of light and slender structures with large spans between support points [1]. These physical characteristics cause their dynamic properties, particularly the modal frequencies, to present values below 10 Hz, which makes them highly susceptible to dynamic loads in this frequency range [2, 3]. However, it has been shown that the normal walking frequency of a pedestrian corresponds to approximately 2 Hz [1], thereby demonstrating the possible occurrence of excessive vibrations resulting from the close coincidence of bridge frequencies and anthropometric loads. This was the case for the Millennium Bridge [4] and the Solferino Bridge [5], which were closed days after their opening because of excessive lateral vibrations caused by pedestrian traffic.

Following these events, standards were developed to govern the design of these types of structures [6–9]. However, none of these fully consider Human Structure Interaction (HSI) and mostly only suggest a minimum modal frequency value and an assessment using a moving ground reaction force (GRF) model [10]. Therefore, it is possible to expect an underestimation of the vibrations produced by human activity [11], triggering rehabilitation and maintenance cost overruns to the initial budget. In this context, the study of HSI plays an important role in the design of pedestrian structures, which is why the development of robust models and methodologies that adequately represent HSI characteristics is of great relevance.

To reliably represent the dynamic behavior of pedestrian bridges under anthropometric loads, it is necessary to analyze the effect of human loads on the dynamic response of the structure and the effect of vibrations on pedestrian gait.

However, this problem is scaled depending on the number of pedestrians, affecting walking conditions such as frequency and step length in individual people [12]; this phenomenon is known as Human-Human Interaction (HHI), and on the other hand, changing the dynamic properties of the coupled human-structure system, in contrast to the empty structure or with low occupancy levels [13–15]. In this paper, we will focus on HSI and consider a single pedestrian in the structure; in that sense, we will disregard the effects of HHI.

To simulate the HSI, several models have been proposed, the simplest of which corresponds to describing the human gait as a time varying equivalent GRF, represented by a Fourier series [16, 17]. However, this basic model does not consider HSI effects. This neglects the influence of the human body on structural dynamics and the impact of structural vibrations on anthropometric loads [18, 19]. Therefore, researchers introduced a model that represents pedestrians as a single-degree-of-freedom (SDoF) dynamic system consisting of a spring, mass, and damper (SMD) in the vertical direction. Many other researchers have developed similar models, known as biodynamic models [14, 20–23], and one or more degrees of freedom have been added with parameters defined by experimental tests [14, 24–29].

The second method used by the authors represents human gait using a mechanical inverted pendulum model (IPM) [30, 31], which consists of two rigid legs connected to a concentrated mass. However, in this model, the representation of GRFs is limited by simply considering single-stance phases during gait [31]. Therefore, the IPM has become sophisticated by incorporating springs into each limb and defining the double stance phase, resulting in a spring-loaded inverted pendulum (SLIP) [32]. Its main limitation is that it overestimates the GRFs in the double stance phases. To improve the SLIP model, the damped bipedal inverted pendulum model (DSLIP) [33, 34] has been proposed as the main option because it has been shown to provide a good approximation in the representation of vertical GRFs. IP, SLIP, and DSLIP models have been incorporated into HSI studies [33, 35, 36]; however, the reliability of GRFs in vibrating structures has not yet been demonstrated [32].

Although these investigations represent an important advance, the main problem lies in the low accuracy of GRFs, due to the simplifications assumed by this type of model, especially the transient, nonstationary condition and the biological variability of human gait [37]. On the other hand, it has been shown that a realistic representation of human gait based on anthropometric characteristics improves the prediction of GRFs and therefore of HSI [38]. In this context, the authors have made advances in the development of biomechanical gait models that consider anthropometric characteristics based on optimisation techniques [39, 40]. Although the previous methodology has, among its advantages, the possibility of including more specific characteristics of people, the problem lies in its high computational requirements. Therefore, the inverse dynamics method has become a very attractive alternative for the development of human gait models based on optimisation techniques [39–41] because it does not require the solution of differential equations, which are responsible for the greatest processing load. However, these models do not consider the support surface motion. In this sense, there is still a need to develop robust models capable of accurately and efficiently predicting HSI characteristics, which will serve as a starting point for the formulation of appropriate standards in the design of pedestrian structures.

In this study, a coupled HSI model involving the dynamics of human and structural systems is proposed. This model is based on the principle that natural processes use as little energy as possible to execute [37, 39]. Therefore, the mechanical energy required to cross a pedestrian bridge is proposed as an objective function. In addition, it includes a set of kinematic, kinetic, and forward constraints that allow it to predict human walking.

2. Human-Structure Interaction Model

The HSI model implemented in this research combines the representation of human gait in the sagittal plane proposed by [39] and the analytical description of a pedestrian bridge (see Figure 1).

2.1. Human System. The movement of the human body on the sagittal plane is represented through a model of 7 rigid elements connected by joints, as proposed by [39]. The upper limbs, head, and torso are combined into a single element called the head-arm trunk (HAT), and each leg contains three elements representing the thigh, shank, and feet. The kinematics of this model are described by a Fourier series representing the angular displacement (θ_i) of ith body segment as a function of the walking frequency (ω_c) due to the periodic nature of the human body movements. The angular displacement is represented by a fifth-order Fourier series as shown in the following equation:

$$\theta_i = a_o + \sum_{n=1}^{5} \left[a_n^{(i)} \cos(n\omega_c t) + b_n^{(i)} \sin(n\omega_c t) \right]. \quad (1)$$

In this equation, n is the order of the truncated Fourier series and its respective coefficients a_o, $a_n^{(i)}$, and $b_n^{(i)}$ are the optimisation parameters as described in Section 2.4. The seven-element model was used in a minimization process, where the objective function was the mechanical energy of the human gait (E_m). This energy is expressed as the integral of the power over the time, and it takes a person to cross a pedestrian bridge or platform, as shown in equation (2). It is important to note that this methodology does not require experimental kinematic information to determine the motion of a human body during a gait cycle because all necessary information is derived from the optimisation process. The anthropometric data used for this model correspond to the anthropometric information presented in [42] and after modified by [39].

$$E_m = \int_0^{T_c} \sum_{i=1}^{7} \left| T_i \left(\omega_p^{(i)} - \omega_d^{(i)} \right) \right| \mathrm{d}t. \quad (2)$$

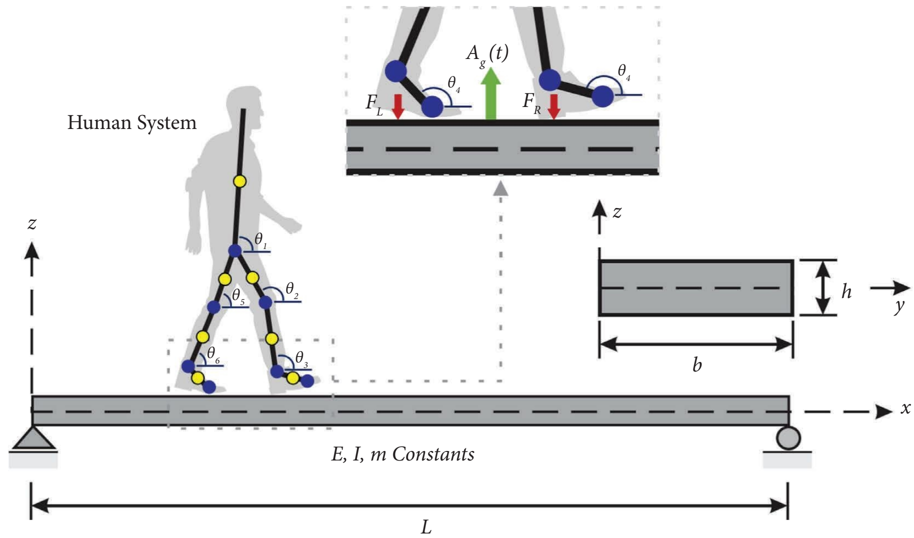

Figure 1: Human structure interaction system.

In equation (2), T_i represents the net torque of element ith and $\omega_p^{(i)}, \omega_d^{(i)}$ represents the angular velocity of each joint proximal and distal element. From the movements of each body segment, the inverse dynamics methodology was used to determine the merge kinetics of the human system using the expressions formulated by [39] (equations (2)–(4)). These equations were used to calculate the reaction forces ($\overrightarrow{F_i}$) and moments (M_i), which were then used to quantify the mechanical energy used during the transit over the structure.

$$\sum \overrightarrow{F_i} = \sum_{i=1}^{7} m_i\left(\overrightarrow{a}_i - \overrightarrow{g} + \overrightarrow{a_g}(t)\right), \tag{3}$$

where m_i and $\overrightarrow{a}_i$ represent the mass and acceleration in the centre mass of ith body element and $\overrightarrow{g}$ is the gravity. Equation (3) was modified to include the action of vibrations generated in the structure ($\overrightarrow{a_g}(t)$) produced by anthropometric loads, thus coupling the merge kinetics of the HSI.

$$\sum M_i = \sum_{i=1}^{7} I_i \alpha_i - \sum_{i=1}^{7}\sum_{k=1}^{n_i} M_{ki}. \tag{4}$$

Likewise, M_{ki} is the moment of the resultant joint force at the kth joint acting on the ith segment, I_i represents the inertia, and α_i corresponds to angular acceleration on the ith body element.

In the literature, there are models such as the SMD or IP, which have been recently validated on rigid surfaces, showing a well behaviour to reproduce the GRFs [32]. However, the IP models present limitations owing to the own simplifications considered, for example, the assumptions of the location of the center of mass for the whole body and the value for the stiffness and damping in the legs. Therefore, the proposed model in this study presents the possibility of including anthropometric data to reduce the uncertainty associated with biological variability, managing to predict the body movements and consequently the GRFs by inverse dynamics, which in turn can be validated by experimental trials. In summary, based on this model, experimental validations could be performed on the two main components of the HSI, such as first, to the effect of anthropic loads on structural vibrations and the second one corresponds to the effect of these vibrations on the human walking behaviour and GRFs.

2.2. Structural System. The flexible structure proposed to carry out the HSI simulation consisted of a simply supported beam with a prismatic section made of normal-weight concrete. The mechanical and dynamic properties of the structure are presented in Table 1. The frequencies for each vertical vibration mode ($f_{\hat{n}}$) were calculated using equation (5). This represents the conditions of a flexible structure susceptible to dynamic loads, with a fundamental frequency close to the pedestrian walking frequency.

$$f_{\hat{n}} = \frac{(\pi\hat{n})^2}{2\pi}\sqrt{\frac{EI}{\overline{m}L^4}}, \tag{5}$$

where E, I, L, and $\overline{m}$ represent the modulus of elasticity of the concrete, the moment of inertia of the section, length, and mass per unit length of the structure, respectively.

The partial differential equation (PDE) is a fourth order that describes the deflection $u(x,t)$ of any point located on the x axis of the beam at a given instant t (equation (6)). Here, $p(x,t)$ represents the load generated by a person walking on a structure, m represents the mass, and c is the coefficient viscous damper.

Table 1: Properties structural system.

Mechanical properties					Dynamics properties			
b(m)	h(m)	L(m)	$\overline{m}$ (kg/m^3)	f_c'(MPa)	f_1(Hz)	f_2(Hz)	f_3(Hz)	ζ(%)
2	0.031	12	2300	28	2.017	8.076	18.152	5

$$\frac{\partial^2}{\partial x^2}\left[EI(x)\frac{\partial^2 u(x,t)}{\partial x^2}\right] + m(x)\frac{\partial^2 u(x,t)}{\partial x^2} + c(x)\frac{\partial u(x,t)}{\partial t} = p(x,t). \quad (6)$$

The PDE was solved using the separation of variables method, which involves modal decomposition, as shown in equation (7). For this case, the vibration modes are described by sinusoidal functions (equation (8)). Equation (9) represents the motion ($Y_{\widehat{n}}$) of the $\widehat{n}$th vibration mode ($\phi_{\widehat{n}}$) in modal coordinates, where the natural frequency ($\omega_{\widehat{n}} = 2\pi f_{\widehat{n}}$) and the damping ratio (ξ) are described using the values from Table 2. The mass ($M_{\widehat{n}}$) and modal loads ($P_{\widehat{n}}$) are characterised by equations (10) and (11), respectively.

$$u(x,t) = \sum_{\widehat{n}=1}^{\infty} \phi_{\widehat{n}}(x) Y_{\widehat{n}}(t), \quad (7)$$

$$\phi_{\widehat{n}}(x) = \sin\left(\frac{\widehat{n}\pi}{L}x\right), \quad (8)$$

$$\ddot{Y}_{\widehat{n}}(t) + 2\xi\omega_{\widehat{n}}\dot{Y}_{\widehat{n}}(t) + \omega_{\widehat{n}}^2 Y_{\widehat{n}}(t) = \frac{P_{\widehat{n}}(t)}{M_{\widehat{n}}}, \quad (9)$$

$$M_{\widehat{n}} = \int_0^L \left[\phi_{\widehat{n}}(x)\right]^2 m(x)\mathrm{d}x, \quad (10)$$

$$P_{\widehat{n}}(t) = \int_0^L \phi_{\widehat{n}}(x) p(x,t)\mathrm{d}x. \quad (11)$$

2.3. Formulation of HSI. Starting from the equations that describe the kinematics and kinetics of the human gait, as presented in Section 2.1, the dynamic systems of human and structure are coupled by incorporating the force induced by walking as a function of time and position in the human system, as shown in equation (12). The left and right foot force transition $D(t)$, Figure 2, is defined as function normalised into 0 to 1, where in single-stance zones, that is, when only one foot is in contact, begin (BGN) to heel contact right (HCR) and toe off left (TOL) to heel contact left (HCL), the function $D(t) = 1$. However, in double stance zones, in the shaded area from HCR to TOL and HCL to toe off right (TOR), $D(t)$ changes linearly from 0 to 1 and from 1 to 0, respectively.

$$\begin{aligned} p(x,t) = &\left[(1 - D(t))\sum_{i=1}^{7} m_i\left(a_i(t) - g + a_g(t)\right)\right]\delta\left(x - x_L(t)\right) \\ &+ \left[D(t)\sum_{i=1}^{7} m_i\left(a_i(t) - g + a_g(t)\right)\right]\delta\left(x - x_R(t)\right), \end{aligned} \quad (12)$$

$$\begin{aligned} x_L(t) &= x_L'(t) + CoP_l(t), \\ x_R(t) &= x_R'(t) + CoP_r(t), \end{aligned} \quad (13)$$

here, $x_L'(t)$ and $x_R'(t)$ in equation (13) represent the positions of the left and right feet, respectively, where $CoP_l(t)$ and $CoP_r(t)$ are the positions of the pressure centres for the left and right feet, respectively. The accelerations induced by the structure owing to the human gait are represented by equation (14), where $a_g(t)$ is calculated based on the positions of the feet and vertical modes of vibration.

$$a_g(t) = \sum_{\widehat{n}=1}^{3}\left[(1 - D(t))\sin\left(\frac{\widehat{n}\pi x_L(t)}{L}\right) + D(t)\sin\left(\frac{\widehat{n}\pi x_R(t)}{L}\right)\right]\ddot{Y}_{\widehat{n}}(t). \quad (14)$$

The applied force of human walking in modal coordinates was obtained by combining equations (10) and (12), and we obtain equation (15)

Table 2: Simulation constraints. Adapted from [39].

Constrain	Lineal	Nonlinear
Range angular motion	$\theta_{\min}^{(i)} \le \theta_i(t) \le \theta_{\max}^{(i)},\ t \in [0, T_c]\ \ (i = 1, 2, \ldots, 7)$	
Relative knee rotation	$\theta_{\min}^{(1)} \le \theta_2(t) - \theta_3(t) \le \theta_{\max}^{(1)}$, $\theta_{\min}^{(2)} \le \theta_4(t) - \theta_3(t) \le \theta_{\max}^{(2)},\ t \in [0, T_c]$	
Foot contact		$y_{\mathrm{tip}}(t) > 0$, during the swing phase $y_{\mathrm{tip}}(t) = 0$, when in contact with the ground
Kinetics		$F_y > 0$ and $-\mu < ([F_x/F_y]) < \mu$, when in contact with the ground
Stride length		$x_{an}(T_c) - x_{an}(0) = V_a T_c$

$T_c = 1/\omega_c$ is the walking period, μ is the coefficient of static friction, y_{tip} is the lowest point of the foot measured from the ground surface, x_{an} is the position of the ankle in the x coordinate, and V_a is the walking speed. The maximum values $\theta_{\max}^{(i)}$ and minimum angular values $\theta_{\min}^{(i)}$ were defined with respect to the limits of the human body, which were defined in [43].

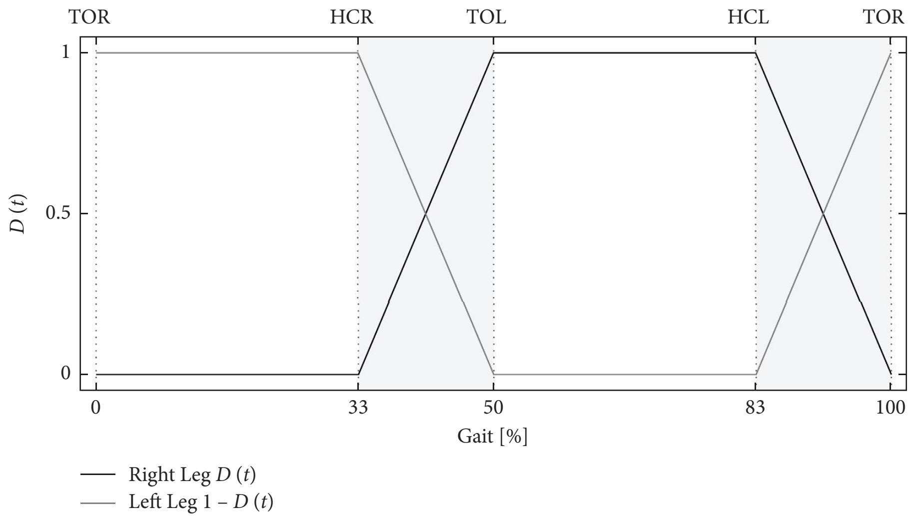

Figure 2: The normalised left and right foot force transition functions during a gait cycle.

$$P_{\hat{n}}(t) = -\left[F_L(t)\sin\left(\frac{\hat{n}\pi x_L(t)}{L}\right) + F_R(t)\sin\left(\frac{\hat{n}\pi x_R(t)}{L}\right)\right] - \left[(1-D(t))m_p\sin\left(\frac{\hat{n}\pi x_L(t)}{L}\right) + D(t)m_p\sin\left(\frac{\hat{n}\pi x_R(t)}{L}\right)\right]a_g(t), \tag{15}$$

$$\ddot{Y}_{\hat{n}}(t) + \frac{m_p}{M_{\hat{n}}}S_{\hat{n}}(t)\left[\sum_{m=1}^{3} S_m(t)\ddot{Y}_{\hat{n}}(t)\right] + 2\zeta_{\hat{n}}\omega_{\hat{n}}\dot{Y}_{\hat{n}}(t) + \omega_{\hat{n}}^2 Y_{\hat{n}}(t) = -\frac{1}{M_{\hat{n}}}\left[F_L(t)\sin\left(\frac{\hat{n}\pi x_L(t)}{L}\right) + F_R(t)\sin\left(\frac{\hat{n}\pi x_R(t)}{L}\right)\right], \tag{16}$$

$$S_{\hat{n}}(t) = (1-D(t))\sin\left(\frac{\hat{n}\pi x_L(t)}{L}\right) + D(t)\sin\left(\frac{\hat{n}\pi x_R(t)}{L}\right), \tag{17}$$

where $F_L(t)$ and $F_R(t)$ correspond to the forces induced by walking on the left and right feet, respectively, without considering the influence of acceleration on the structure. The total mass of the human system is denoted by $m_p = \sum_{i=1}^{7} m_i$.

Substituting equation (15) into equation (9), the modal coordinate equation for solving the HSI model, given by equation (16), can be expressed in matrix form, as shown in equation.

$$\left[M + m_p S^T(t)S(t)\right]\ddot{Y}(t) + C\dot{Y}(t) + KY(t) = -\Phi(x_L(t))F_L(t) - \Phi(x_R(t))F_R(t). \tag{18}$$

In equation (18), M represents the modal mass, C represents the damping, and K represents the stiffness of the human-structure system, as given by equations (19)–(21), respectively.

$$M = \begin{bmatrix} M_1 & & & \\ & M_2 & & \\ & & \ddots & \\ & & & M_{\widehat{n}} \end{bmatrix}, \tag{19}$$

$$C = \begin{bmatrix} 2\zeta_1\omega_1 M_1 & & & \\ & 2\zeta_2\omega_2 M_2 & & \\ & & \ddots & \\ & & & 2\zeta_{\widehat{n}}\omega_{\widehat{n}} M_{\widehat{n}} \end{bmatrix}, \tag{20}$$

$$K = \begin{bmatrix} \omega_1^2 M_1 & & & \\ & \omega_2^2 M_2 & & \\ & & \ddots & \\ & & & \omega_{\widehat{n}}^2 M_{\widehat{n}} \end{bmatrix}. \tag{21}$$

2.4. Optimization. The optimisation process employed an interior-point optimisation algorithm implemented in MATLAB's fmincon function. Although fmincon interior-point is a local optimizer, the large number of linear and nonlinear constraints means that the area of feasible solutions is consequently limited. In this sense, it can be expected that a local solution is close to the global minimum and that the angles and forces will be similar to those corresponding to the global minimum. This has been discussed by other authors including Ren et al. [39]. Moreover, as the initial coefficients (x_0) used are those corresponding to gait on a rigid surface, it can be expected that the solution obtained, although possibly suboptimal, will be representative of gait motion patterns that are subject to HSI effects. The computations were carried out on a computer with the following specifications: Windows 11 Pro 64 bit operating system, AMD Ryzen 3900X processor running at 3.97 GHz and 32.0 GB RAM.

The objective of the optimisation was to predict the angular kinematics of each body segment by determining the coefficients of a Fourier series of order five, as described in equation (1). The primary goal was to minimise the mechanical energy expended by the human system during the traversal of the structure, as indicated in equation (2). To ensure the feasibility of the solution, various constraints were considered, as listed in Table 2. These constraints include limitations on joint angles to prevent hyperextensions, requirements for positive vertical contact forces at the feet, adherence to friction coefficients for horizontal components, and the need to maintain at least one foot in contact with the structure throughout the gait cycle. Meanwhile, equation (18), which describes the merge HSI, was solved using the fourth and fifth-order Runge–Kutta method in Ode45 function of MATLAB because, among its options, it allows the solution of ordinary differential equations with non-constant coefficients.

Throughout the optimisation process, the initial values for the gait parameters, such as average walking speed, walking frequency, and double support duration, were specified. These initial values served as starting points for the optimisation algorithm, which iteratively refined the parameters to determine optimal gait characteristics. This optimisation approach aims to develop a biomechanical model that accurately predicts human gait on a flexible structure, while minimizing energy expenditure and satisfying defined constraints.

3. Results and Discussion

In this section, the results obtained from a simulation of the interaction between the human system and a flexible structure are presented. Detailed analyses were conducted to assess the impact of the HSI on various aspects, including the kinematics of the human body, vertical walking forces, and dynamic response of the reference structure.

An HSI simulation was performed with an 80 kg test subject walking along the reference structure at a walking frequency of $\omega_c = 2Hz$ and stride length of 1.5 m (two steps). Regarding foot stance times during a gait cycle, the authors agree that the duration of the dual stance phases (HCR to TOL and HCL to TOR) are in a range between 32% and 42% of the total gait cycle [44–47]. In this order, following the way of Ren et al. [39], the double support duration was defined in the ranges between 33 to 50 and 83 to 100% (see Figure 2). The simulation processing time was approximately two minutes, with 162 iterations, resulting in a minimum value of $E_m = 201\,J$ for the cost function. The optimal coefficients of the Fourier series, which describe the variation in the absolute angles of each body segment during pedestrian passage, are presented in Table 3. These coefficients allow for a precise and realistic representation of the kinematics of the human body in response to the vibration of the structure ($a_g(t)$).

In Figures 3 and 4, the dotted black line and the solid blue line correspond to the results of the gait model proposed in this research for rigid surface and the results considering HSI, respectively. On the other side, the shaded areas refer to the statistical analysis of the experimental data presented in [48, 49], where the upper and lower limits are given by the mean ± two standard deviations.

The relative angles for the hip, knee, and ankle joints, considering the effects of HSI, are shown in Figure 3. These angles were contrasted with experimental data from an optical motion capture OptiTrack system recorded by [48], showing good similarity in magnitude and shape and the differences are attributed to the stiffness of the elements of the human model, which is a characteristic of this type of model [50], confirming that the solution of the optimisation process corresponds to a normal gait pattern. The percentage comparisons with their counterparts on a rigid surface showed differences of 8, 7, and 5%, respectively. Similarly, comparisons were made for the vertical forces with and without considering the effects of the HSI. These were compared with force tests during gait recorded with a pair of insole pressure sensors (Stridalyzer Insight developed by ReTiSense) [49]. The results show that the forces predicted by the model are mostly within the range established by the experimental data. Figure 4 displays the vertical force along

Table 3: Fourier series coefficients.

Element	θ_i	0	1	2	3	4	5
HAT	a_n	1.51	54.04	−42.89	2.67	−3.54	1.44
	b_n		−20.34	−12.1	5.87	23.93	0.7
Thigh	a_n	1.81	156.86	−83.14	17.14	15.1	10.52
	b_n		−139.29	−20.91	−16.06	−0.69	6.73
Shank	a_n	1.31	453.1	−92.95	−9.66	14.76	−6.54
	b_n		−307.1	−36.66	75.73	−14.44	−12.49
Foot	a_n	2.38	614.96	−261.64	39.6	−12.79	0.69
	b_n		−386.47	−102.11	138.16	−35.6	5.69

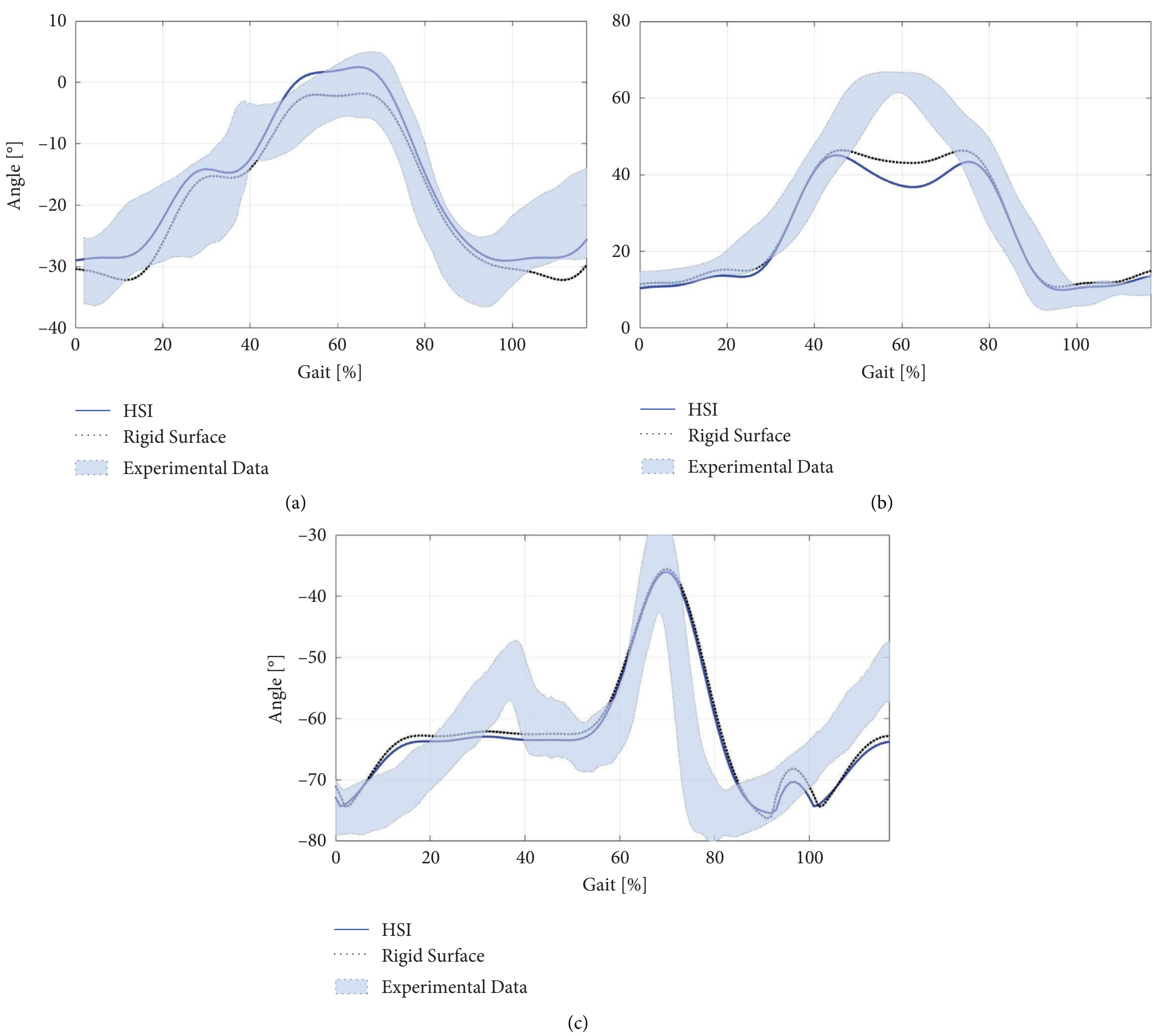

Figure 3: Relative angles during human gait. (a) Hip, (b) knee, and (c) ankle.

the pedestrian bridge, highlighting the gait cycle near the centre span, where the influence of the HSI on the GRFs is observed with a difference of 10%. These changes were significant, with an increase in magnitude of approximately 30 N, demonstrating the effects of HSI on the human system. This can be primarily attributed to the flexibility of the structure and its frequency coinciding with the walking frequency.

In Figure 3, although the general shape of the angles coincides with the experimental measurements during the

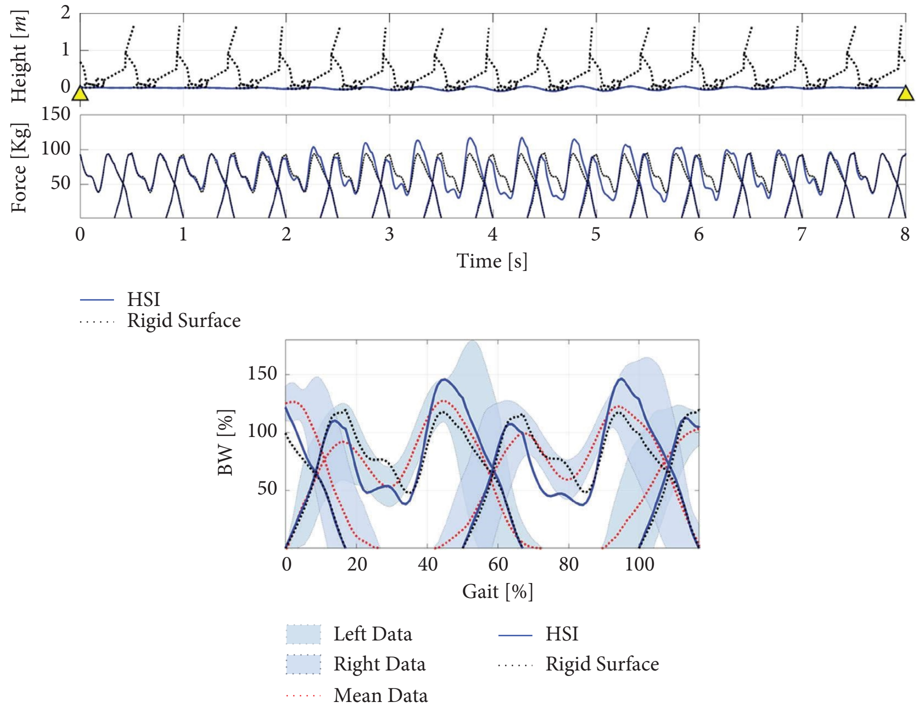

Figure 4: Ground reaction vertical forces during human gait.

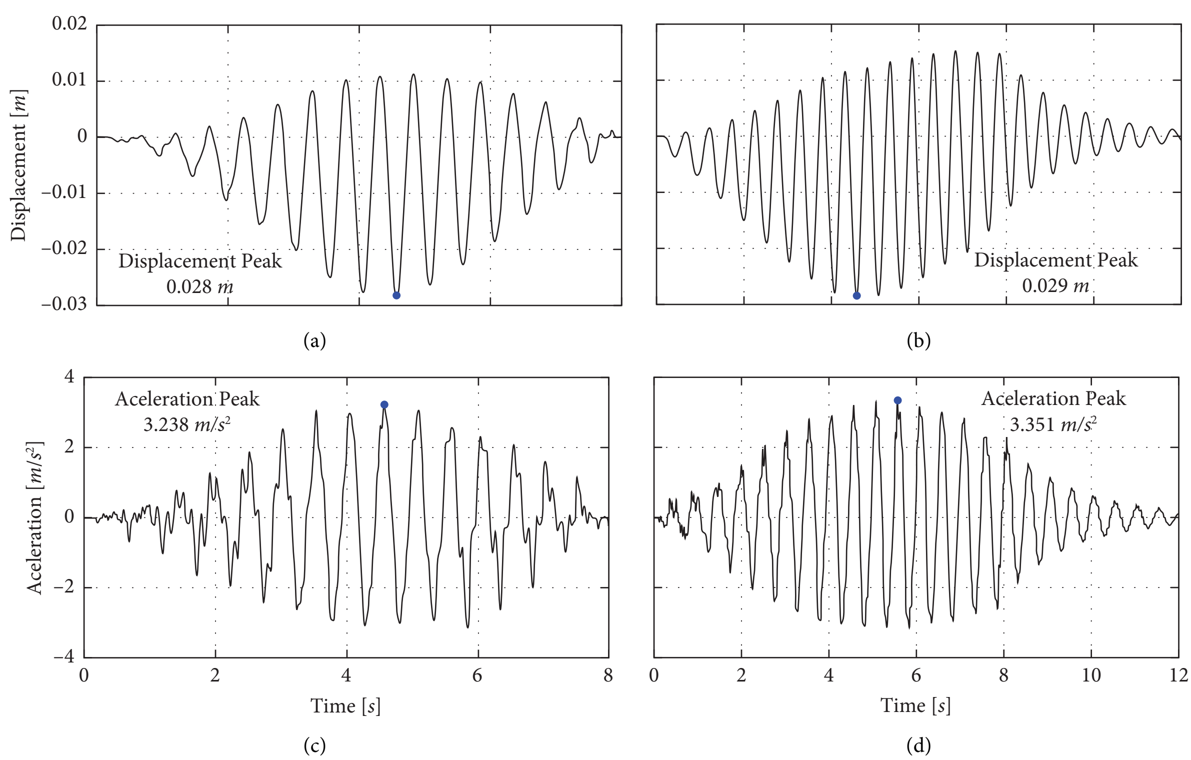

Figure 5: Response dynamics structural system. (a) Displacement contact point $D_g(t)$, (b) displacement middle point center length bridge, (c) acceleration contact point $a_g(t)$, and (d) acceleration middle center.

gait cycle [48] being within the experimental reliability zone at 95.5, 82, and 81% for the pelvis, knee, and ankle angles, respectively. The differences are attributed to the simplification of the upper body elements into a HAT element and the lack of transverse rotation of the pelvis in the model as mentioned by Ren et al. [39]. Similarly, for the

GRFs in Figure 4, the differences with the experimental data [49] are attributed to the simplification of the model and, as mentioned in the literature, to the stiffness of the elements that compose the human model [50].

The acceleration at the contact point ($a_g(t)$) during HSI is shown in Figure 5(c). Acceleration levels of 3 m/s^2 were recorded, with a peak of 3.238 m/s^2. These accelerations are significant enough to considerably alter the walking pattern and, consequently, result in a significant increase in the GRFs of the human system and response of the structure. This pattern is repeated until a pedestrian crosses the structure.

Finally, Figures 5(a) and 5(d) show the overall response of the structural system to anthropometric loads, considering the effects of HSI. Figures 5(b) and 5(d) show the displacements and accelerations at the centre of the span, reaching a maximum of 0.029 m and 3.351 m/s^2, respectively, highlighting the amplification in the dynamic response of the structure owing to its resonance with the anthropic loads. These results validate the capability of the developed models to represent HSI.

4. Conclusions

In this study, a vertical HSI model for pedestrian bridges was developed, which consisted of a simplified biomechanical model of human gait with seven rigid elements and a structural system represented by a simply supported beam. The primary objective of this model is to minimise the average mechanical energy required for a gait cycle to cross a pedestrian bridge. The HSI effects were effectively captured by employing a combination of inverse dynamics to calculate the kinematics and kinetics of human gait and direct dynamics to solve the differential equations governing the structural response under anthropometric loads, and the HSI effects were effectively captured.

The estimation of the body segment movements and ground reaction forces was based on three essential gait characteristics: average walking speed, frequency, and stride length. Natural body movements were allowed without imposing any artificial constraints except for physically unrealistic hyperextensions. The resulting body segment movements, as depicted in Figure 3, closely resemble normal patterns and remain within the joint limits reported in the relevant literature, such as [43]. Moreover, the minimum mechanical energy obtained in this model is lower than that reported by [39], which can be attributed to the inclusion of the HSI effects.

The utilisation of inverse dynamics, as opposed to direct dynamics, offers several advantages, including computational efficiency, which is crucial for optimisation-based predictive models. The computational cost was mainly associated with solving the differential equations governing the structural system. However, by combining the direct and inverse dynamics, the overall execution time for each optimisation iteration was significantly reduced.

The proposed model effectively simulates the kinematics and kinetics of human gait and accurately captures the dynamic response of structures subjected to HSI effects. It is important to note that the vertical force pattern (see Figure 4) exhibits a different number of peaks compared to the existing force patterns reported in the literature. However, this discrepancy is commonly observed in models with high leg stiffness at low walking speeds, where a greater number of force peaks are generated as the walking speed decreases [50].

The simulation results of the HSI demonstrate the potential of this modelling approach to represent HSI effects on pedestrian bridges, making it a viable tool for evaluating and understanding the impact of HSI.

Comparing the simulation results between walking on a rigid surface and walking on a bridge governed by partial differential equations, notable changes in the contact forces induced by pedestrians traversing the structure were observed. Specifically, an increase of 12% in the vertical force highlights the influence of the HSI effects on the contact forces and their implications for the structural response.

Data Availability

The data that support the findings of this study are available from the corresponding author upon reasonable request.

Conflicts of Interest

The authors declare that they have no conflicts of interest.

Acknowledgments

This work is part of the research projects: (1) formation and insertion of high-level human capital for the regions biennium 2021–2022, Universidad del Valle, Valle del Cauca, CT 15-2021 FAN SGR—BPIN: 2021000100099. (2) Wind Microzonification of the City of Santiago de Cali, Phase I: Wind Tunnel Evaluation of Wind Speed Profiles, C.I. 21130. The authors would like to express their gratitude to the Universidad del Valle and the Ministerio de Ciencia Tecnología e Innovación (Minciencias), which financed the project.

References

[1] S. Živanović, A. Pavic, and P. Reynolds, "Vibration serviceability of footbridges under human-induced excitation: A literature review," *Journal of Sound and Vibration*, vol. 279, no. 1-2, pp. 1–74, 2005.

[2] J. Anderson Sánchez, D. Gómez, and P. Thomson, "Analysis of human-structure interaction in footbridges in Santiago de Cali," *DYNA (Colombia)*, vol. 80, pp. 86–94, 2013.

[3] A. R. Ortiz, D. Gómez, and P. Thomson, "Efectos de la interacción humano-estructura en las propiedades dinámicas de una tribuna," *Ingeniería y Competitividad*, vol. 14, no. 1, pp. 63–73, 1969.

[4] P. Dallard, A. J. Fitzpatrick, A. Flint, S. Le Bourva, A. Low, and M. Willford, "The London Millennium footbridge," *Structural Engineer*, vol. 79, no. 22, pp. 17–21, 2001.

[5] E. T. Ingólfsson, C. T. Georgakis, and J. Jönsson, "Pedestrian-induced lateral vibrations of footbridges: a literature review," *Engineering Structures*, vol. 45, pp. 21–52, 2012.

[6] T. M. Murray, E. E. Ungar, and D. Brad Davis, "Vibrations of steel-framed structural systems due to human activity," in *Steel Design Guide*, American Institute of Steel Construction, Chicago, IL, USA, 2nd edition, 2016.
[7] *Eurocode 5, Design of Timber Structures–Part 2: Bridges*, European Committee of Standardization, Brussels, Belgium, 2004.
[8] British Standards Institution BSI, "UK national annex to Eurocode 1: Actions on structures-Part 2: traffic loads on bridges," European Committee of Standardization, London, UK, 2003.
[9] A. C. Ingeniería Sísmica, *Reglamento Colombiano de Construcción Sismo Resistente (NSR-10)*, Asociación Colombiana de Ingeniería Sísmica (ACIS), Bogotá, Colombia, 2010.
[10] E. Shahabpoor, A. Pavic, and V. Racic, "Interaction between walking humans and structures in vertical direction: a literature review," *Shock and Vibration*, vol. 2016, Article ID 3430285, 22 pages, 2016.
[11] S. Živanović, A. Pavić, and E. T. Ingólfsson, "Modeling spatially unrestricted pedestrian traffic on footbridges," *Journal of Structural Engineering*, vol. 136, no. 10, pp. 1296–1308, 2010.
[12] X. Wei, K. Van Nimmen, G. De Roeck, and P. Van den Broeck, "A simplified method to account for human-human interaction in the prediction of pedestrian-induced vibrations," *Structural Control and Health Monitoring*, vol. 28, no. 7, 2021.
[13] E. Ahmadi, C. Caprani, S. Živanović, N. Evans, and A. Heidarpour, "A framework for quantification of human-structure interaction in vertical direction," *Journal of Sound and Vibration*, vol. 432, pp. 351–372, 2018.
[14] F. T. da Silva, H. M. B. F. Brito, and R. L. Pimentel, "Modeling of crowd load in vertical direction using biodynamic model for pedestrians crossing footbridges," *Canadian Journal of Civil Engineering*, vol. 40, no. 12, pp. 1196–1204, 2013.
[15] F. Venuti, V. Racic, and A. Corbetta, "Modelling framework for dynamic interaction between multiple pedestrians and vertical vibrations of footbridges," *Journal of Sound and Vibration*, vol. 379, pp. 245–263, 2016.
[16] E. Ahmadi, C. Caprani, S. Živanović, and A. Heidarpour, "Vertical ground reaction forces on rigid and vibrating surfaces for vibration serviceability assessment of structures," *Engineering Structures*, vol. 172, pp. 723–738, 2018.
[17] C. C. Caprani and E. Ahmadi, "Formulation of human–structure interaction system models for vertical vibration," *Journal of Sound and Vibration*, vol. 377, pp. 346–367, 2016.
[18] B. Lin, Q. Zhang, F. Fan, and S. Shen, "Reproducing vertical human walking loads on rigid level surfaces with a damped bipedal inverted pendulum," *Structures*, vol. 33, pp. 1789–1801, 2021.
[19] Z. Han and S. Huang, "The influence of human-structure interaction on structural dynamic properties," in *IOP Conference Series: Earth and Environmental Science*, IOP Publishing Ltd, Bristol, UK, 2021.
[20] E. Shahabpoor, A. Pavic, and V. Racic, "Identification of mass-spring-damper model of walking humans," *Structures*, vol. 5, pp. 233–246, 2016.
[21] L. Wang, S. Nagarajaiah, W. Shi, and Y. Zhou, "Semi-active control of walking-induced vibrations in bridges using adaptive tuned mass damper considering human-structure-interaction," *Engineering Structures*, vol. 244, Article ID 112743, 2021.
[22] M. Schubert Pfeil, W. Diniz Varela, and N. de Paula Amador da Costa, "Experimental calibration of a one degree of freedom biodynamic model to simulate human walking-structure interaction," *Engineering Structures*, vol. 262, Article ID 114330, 2022.
[23] D. Colmenares, A. Andersson, and R. Karoumi, "An analytical solution of the maximum response of the coupled multiple parallel modulated pedestrian-bridge system," *Structures*, vol. 57, Article ID 105160, 2023.
[24] J. Lou, M. Zhang, and J. Chen, "Identification of stiffness, damping and biological force of SMD model for Human walking," in *Proceedings of the Society for Experimental Mechanics Series*, pp. 331–337, Springer, New York, NY, USA, January 2015.
[25] K. Van Nimmen, K. Maes, S. Živanović, G. Lombaert, G. De Roeck, and P. Van den Broeck, "Identification and modelling of vertical human-structure interaction," in *Proceedings of the Society for Experimental Mechanics Series*, pp. 319–330, Springer, New York, NY, USA, February 2015.
[26] M. Zhang, C. T. Georgakis, and J. Chen, "Biomechanically excited SMD model of a walking pedestrian," *Journal of Bridge Engineering*, vol. 21, no. 8, 2016.
[27] H. Wang, J. Chen, and J. M. W. Brownjohn, "Parameter identification of pedestrian's spring-mass-damper model by ground reaction force records through a particle filter approach," *Journal of Sound and Vibration*, vol. 411, pp. 409–421, 2017.
[28] K. Van Nimmen, P. Van Den Broeck, and G. Lombaert, "Inverse identification of the pedestrian characteristics governing human-structure interaction," in *Proceedings of the X International Conference on Structural Dynamics, EURODYN 2017*, pp. 2889–2894, Elsevier Ltd, Amsterdam, Netherlands, December 2017.
[29] E. Ahmadi, C. C. Caprani, and A. Heidarpour, "An equivalent moving force model for consideration of human-structure interaction," *Applied Mathematical Modelling*, vol. 51, pp. 526–545, 2017.
[30] P. Mahmoodi, R. S. Ransing, and M. I. Friswell, "A novel mathematical formulation for predicting symmetric passive bipedal walking motion with unbalanced masses," *Applied Mathematical Modelling*, vol. 40, no. 5–6, pp. 3895–3906, 2016.
[31] M. Bocian, J. H. G. Macdonald, and J. F. Burn, "Biomechanically inspired modeling of pedestrian-induced vertical self-excited forces," *Journal of Bridge Engineering*, vol. 18, no. 12, pp. 1336–1346, 2013.
[32] B. Lin, S. Zhang, S. Živanović, Q. Zhang, and F. Fan, "Verification of damped bipedal inverted pendulum model against kinematic and kinetic data of human walking on rigid-level ground," *Mechanical Systems and Signal Processing*, vol. 200, Article ID 110561, 2023.
[33] J. W. Qin, S. S. Law, Q. S. Yang, and N. Yang, "Pedestrian-bridge dynamic interaction, including human participation," *Journal of Sound and Vibration*, vol. 332, no. 4, pp. 1107–1124, 2013.
[34] B. Lin, S. Zivanovic, Q. Zhang, and F. Fan, "Implementation of damped bipedal inverted pendulum model of pedestrian into FE environment for prediction of vertical structural vibration," *Structures*, vol. 48, pp. 523–532, 2023.
[35] H. Yang, B. Wu, J. Li, Y. Bao, and G. Xu, "A spring-loaded inverted pendulum model for analysis of human-structure interaction on vibrating surfaces," *Journal of Sound and Vibration*, vol. 522, Article ID 116727, 2022.
[36] B. Lin, Q. Zhang, F. Fan, and S. Shen, "A damped bipedal inverted pendulum for human–structure interaction

analysis," *Applied Mathematical Modelling*, vol. 87, pp. 606–624, 2020.

[37] D. A. Winter, *Biomechanics and Motor Control of Human Movement*, John Wiley and Sons, Inc, Hoboken, NJ, USA, 2009.

[38] B. R. Whittington and D. G. Thelen, "A simple mass-spring model with roller feet can induce the ground reactions observed in human walking," *Journal of Biomechanical Engineering*, vol. 131, no. 1, Article ID 011013, 2009.

[39] L. Ren, R. K. Jones, and D. Howard, "Predictive modelling of human walking over a complete gait cycle," *Journal of Biomechanics*, vol. 40, no. 7, pp. 1567–1574, 2007.

[40] Y. Xiang, J. S. Arora, and K. Abdel-Malek, "Physics-based modeling and simulation of human walking: a review of optimization-based and other approaches," *Structural and Multidisciplinary Optimization*, vol. 42, no. 1, pp. 1–23, 2010.

[41] H. Salehi, L. Ren, and D. Howard, "A fast inverse dynamics model of walking for use in optimisation studies," *Computer Methods in Biomechanics and Biomedical Engineering*, vol. 19, no. 11, pp. 1201–1209, 2016.

[42] P. de Leva, "Adjustments to Zatsiorsky-Seluyanov's segment inertia parameters," *Journal of Biomechanics*, vol. 29, no. 9, pp. 1223–1230, 1996.

[43] J. Panero and M. Zelnik, *Human Dimension and Interior Space: A Source Book of Design Reference Standards*, Random House US, New York, NY, USA, 2014.

[44] T. P. Andriacchi, J. A. Ogle, and J. O. Galante, "Walking speed as a basis for normal and abnormal gait measurements," *Journal of Biomechanics*, vol. 10, no. 4, pp. 261–268, 1977.

[45] K. Jordan, J. H. Challis, and K. M. Newell, "Walking speed influences on gait cycle variability," *Gait & Posture*, vol. 26, no. 1, pp. 128–134, 2007.

[46] A. Kharb, V. Saini, Y. Jain, and S. Dhiman, "A review of gait cycle and its parameters," *The International Journal of Computational Engineering and Management*, vol. 13, 2011.

[47] B. Castillo, J. Marulanda, and P. Thomson, "Experimental evaluation of pedestrian-induced multiaxial gait loads on footbridges: Effects of the structure-to-human interaction by lateral vibrating platforms," *Sensors*, vol. 24, no. 8, p. 2517, 2024.

[48] B. Castillo, C. Riascos, and J. M. Franco, "Assessing spatiotemporal behavior of human gait: a comparative study between low-cost smartphone-based mocap and optitrack systems," *Expedition Technology*, vol. 13, 2024.

[49] B. Castillo, A. L. Arango, J. Marulanda, and P. Thomson, "Comprehensive experimental analysis of the vibration serviceability due to dynamic interaction between footbridge with accurate multi-axial dynamic sensitivity and human-induced gait loads," *Mendeley Data*, vol. 1, 2024.

[50] H. Geyer, A. Seyfarth, and R. Blickhan, "Compliant leg behaviour explains basic dynamics of walking and running," *Proceedings of the Royal Society B: Biological Sciences*, vol. 273, no. 1603, pp. 2861–2867, 2006.